

The Clustering and Host Halos of Galaxy Mergers at High Redshift

Andrew R. Wetzel¹, J.D. Cohn², Martin White^{1,3}

¹*Department of Astronomy, University of California, Berkeley, CA 94720, USA*

²*Space Sciences Laboratory, University of California, Berkeley, CA 94720, USA*

³*Department of Physics, University of California, Berkeley, CA 94720, USA*

October 2008

ABSTRACT

High-resolution simulations of cosmological structure formation indicate that dark matter substructure in dense environments, like groups and clusters, may survive for a long time. These dark matter subhalos are the likely hosts of galaxies. We examine the small-scale spatial clustering of subhalo major mergers at high redshift using high-resolution N-body simulations of cosmological volumes. Recently merged, massive subhalos exhibit enhanced clustering on scales $\sim 100 - 300h^{-1}$ kpc, relative to all subhalos of the same infall mass, for a short time after a major merger (< 500 Myr). The small-scale clustering enhancement is smaller for lower mass subhalos, which also show a deficit on scales just beyond the excess. Halos hosting recent subhalo mergers tend to have more subhalos; for massive subhalos the excess is stronger and it tends to increase for the most massive host halos. The subhalo merger fraction is independent of halo mass for the scales we probe. In terms of satellite and central subhalos, the merger increase in small-scale clustering for massive subhalos arises from recently merged massive central subhalos having an enhanced satellite population. Our mergers are defined via their parent infall mass ratios. Subhalos experiencing major mass gains also exhibit a small-scale clustering enhancement, but these correspond to two-body interactions leading to two final subhalos, rather than subhalo coalescence.

Key words: cosmology:theory – methods:N-body simulations – galaxies:halos – galaxies:interactions

1 INTRODUCTION

A wealth of high redshift galaxy data is now accumulating, and many of the members in the resultant galaxy zoo are thought arise from galaxy mergers: quasars (Carlberg 1990), Lyman Break Galaxies (LBG; see Giavalisco 2002, for review), submillimeter galaxies (SMG; see Blain et al. 2002, for review), ultra-luminous infrared galaxies (ULIRG; see Sanders & Mirabel 1996, for review) and starburst and starburst remnant galaxies (e.g., Barnes & Hernquist 1991; Noguchi 1991). Observational samples of these objects at $z \gtrsim 1$ are growing large enough to produce statistical measurements of clustering which can be compared to candidates in numerical simulations (e.g. Giavalisco et al. 1998; Blain et al. 2004; Croom et al. 2005; Ouchi et al. 2005; Cooray & Ouchi 2006; Hennawi et al. 2006; Kashikawa 2006; Lee et al. 2006; Scott et al. 2006; Coil et al. 2007; Gawiser et al. 2007; Shen et al. 2007; Francke et al. 2008; Myers et al. 2008; Yamauchi et al. 2008; Yan et al. 2008; Yoshida et al. 2008).

In high resolution dark matter simulations, overdense, self-bound, dark matter substructures in dense en-

vironments can survive for a long time (Tormen 1997; Tormen et al. 1998; Ghigna et al. 1998; Klypin et al. 1999; Moore et al. 1999). These “subhalos” are thought to be the hosts of galaxies, and indeed the identification of galaxies with subhalos reproduces many galaxy properties (e.g., Springel et al. 2001, 2005; Zentner et al. 2005; Bower et al. 2006; Conroy et al. 2006; Vale & Ostriker 2006; Wang et al. 2006). The complex dynamics of subhalos may thus be a good proxy for those of galaxies themselves, suggesting that galaxy mergers can be identified with subhalo mergers within simulations. We will use the terms galaxy and subhalo interchangeably hereon. Measurements of subhalo mergers can provide a quantitative reference for the identification of merger related objects in observations and can aid in the correct interpretation of clustering measurements.

One question of particular interest is whether small-scale clustering can probe merger activity. There has been much recent discussion of a “small-scale clustering enhancement” of galaxy subpopulations in simulations and observations, but several differing definitions of “enhancement” exist, mostly stemming from different choices of reference.

For instance, small-scale enhancement has been used to describe clustering stronger than a power law extrapolated from larger scales, or clustering stronger than that of dark matter at small scales. However both of these behaviors are seen in non-merging samples. Luminous Red Galaxies in SDSS are not thought to be associated with (recent) mergers, yet their correlation function is much steeper than the dark matter on scales of several hundred kpc (Masjedi et al. 2006). One expects objects which populate halos more massive than M_* (the characteristic non-linear mass) will have an upturn in their correlation function on scales below the virial radius of the M_* halos since at this scale the clustering is dominated by pairs of objects within the same halo and the mass function is very steep (e.g., Seljak 2000; Peacock & Smith 2000). Quasars (thought to be associated with mergers) do exhibit a sharp upturn in clustering on very small scales ($25 - 50 h^{-1}\text{kpc}$) at $z \approx 1 - 3$ (Hennawi et al. 2006; Myers et al. 2008), but a comparison with galaxy clustering measurements at these scales and redshifts is lacking.¹ On slightly larger scales, low z quasar clustering observations show no excess above a power law (e.g. Padmanabhan et al. 2008, and discussion therein).

On the other hand, merger related clustering effects are not unexpected. Recently, various authors have shown that the large-scale clustering of dark matter halos depends on their formation histories (known as “assembly bias”; e.g., Sheth & Tormen 2004; Gao et al. 2005; Wechsler et al. 2006), and in particular, on recent halo merger activity (“merger bias”; Scannapieco & Thacker 2003; Wetzel et al. 2007).² Any such history or merger dependent clustering breaks the usually assumed direct link between large-scale clustering amplitude and halo mass. Analytical modeling of the small-scale clustering of quasars has been compared to observations, assuming that quasars are mergers and that mergers occur in denser environments (Hopkins et al. 2008).

In this paper, we focus on the small-scale clustering of subhalo mergers and the relation to their host halos. We use dark matter simulations to compare the small-scale clustering of recently merged subhalos at high redshifts to the clustering of the general subhalo population of the same infall mass. To interpret our results, we relate the merged subhalos to their host dark matter halos using the formalism of the halo model (Seljak 2000; Peacock & Smith 2000; Cooray & Sheth 2002), examining the dependence of subhalo mergers both on their host halo masses and their halo radial distribution profiles.

In §2 we briefly describe the simulations and summarize the main properties of subhalo tracking and merger definitions as detailed in Wetzel et al. (2008), hereafter called Paper I. In §3 we compare the small-scale clustering of the recently merged and full population of subhalos. We also describe results for the alternate mass gain merger definition. In §4 we use the framework of the halo model to identify contributions to merger clustering and to understand the relation of subhalo mergers to their host dark matter halos.

We note properties of merger pairs in §5, and we summarize and discuss our results in §6.

2 NUMERICAL TECHNIQUES AND MERGER DEFINITIONS

2.1 Simulations and Subhalo Tracking

Our simulation and subhalo finding and tracking details are discussed extensively in Paper I; we summarize only the main features here. We use two dark matter only N-body TreePM (White 2002) simulations of 800^3 and 1024^3 particles in periodic cubes with side lengths $100 h^{-1}\text{Mpc}$ and $250 h^{-1}\text{Mpc}$, respectively. For our ΛCDM cosmology ($\Omega_m = 0.25$, $\Omega_\Lambda = 0.75$, $h = 0.72$, $n = 0.97$ and $\sigma_8 = 0.8$, in agreement with a wide array of observations (e.g., Smoot et al. 1992; Tegmark et al. 2006; Reichardt et al. 2008; Komatsu et al. 2008), this results in particle masses of $1.4 \times 10^8 h^{-1}M_\odot$ ($1.1 \times 10^9 h^{-1}M_\odot$) and a Plummer equivalent smoothing of $4 h^{-1}\text{kpc}$ ($9 h^{-1}\text{kpc}$) for the smaller (larger) simulation. Outputs were spaced every 50 Myr (~ 100 Myr) for the smaller (larger) simulation, from $z \sim 5$ to 2.5. Additional outputs from the smaller simulation were retained at lower redshift, spaced every ~ 200 Myr down to $z = 0.6$, below which stopped our analysis as we no longer fairly sample a cosmological volume.

We find subhalos (and sometimes subhalos in subhalos) by first generating a catalog of halos using the Friends-of-Friends (FoF) algorithm (Davis et al. 1985) with a linking length of $b = 0.168$ times the mean inter-particle spacing. We keep all groups that have more than 32 particles, and halo masses quoted below are these FoF masses. Within these “(host) halos” we then identify “subhalos” as gravitationally self-bound aggregations of at least 20 particles bounded by a density saddle point, using a new implementation of the *Subfind* algorithm (Springel et al. 2001). The central subhalo is the subhalo with the densest particle in its host halo and it includes all halo matter not assigned to satellite subhalos. Subhalo and halo positions are those of their densest particle.

Each subhalo is given a unique child at a later time, based on its 20 most bound particles. We track subhalo histories across four consecutive outputs at a time since subhalos can briefly disappear during close passage with another subhalo, i.e. “fly-by’s”. Additionally, at these redshifts, the distinction between a central and satellite subhalo is often not clear-cut, especially for halos undergoing rapid merger activity which are highly disturbed and aspherical. In particular, our tracking also can produce “switches”: if a satellite subhalo becomes denser than its central subhalo, it becomes the central while the central becomes a satellite, often switching back in the next output.

We assign to a subhalo its mass when it fell into its current host (i.e., when it was last a central subhalo), M_{inf} . Subhalo infall mass has been shown to correlate with galaxy stellar mass (Vale & Ostriker 2006; Wang et al. 2006; Yang et al. 2008).³ If two satellite subhalos merge, their

¹ It is not clear how to interpret a galaxy clustering measurement on scales smaller than the galactic radius.

² See also Furlanetto & Kamionkowski (2006) for analytic estimates, Percival et al. (2003) for a simulation limit on the effect, Croton et al. (2007); Tinker et al. (2008) for halo assembly bias applied to galaxy clustering.

³ As has subhalo maximum circular velocity at infall, $V_{\text{c,inf}}$ (Conroy et al. 2006; Berrier et al. 2006). We compare M_{inf} and $V_{\text{c,inf}}$ in detail in Paper I.

satellite child is given the sum of their infall masses. During a switch, when a satellite becomes a central, it would acquire all halo mass not bound in other subhalos. To avoid these strong fluctuations appearing in M_{inf} , a central subhalo is assigned its halo's current self bound mass only if it was a central in the same halo in the previous output. If a central was a satellite or a central in a different (smaller) halo in the previous output, it is assigned the sum of its parents' M_{inf} .

We select subhalos with $M_{\text{inf}} > 10^{12} h^{-1} M_{\odot}$ in the larger simulation and scale down to $M_{\text{inf}} > 10^{11} h^{-1} M_{\odot}$ in the smaller, higher resolution simulation, by requiring consistency between the two simulations in their overlap regime.⁴ Halos of mass 10^{11} (10^{12}) $h^{-1} M_{\odot}$ cross below M_* , the characteristic mass of collapse, at $z = 1.5$ ($z = 0.8$), so we probe $M > M_*$ subhalos for much of the redshift range we consider. We also expect our sample of $M_{\text{inf}} > 10^{12} h^{-1} M_{\odot}$ subhalos to approximately correspond to $L \gtrsim L_*$ galaxies at the redshifts we examine (see, e.g., Conroy & Wechsler 2008, for halo-galaxy mass relation based on abundance matching). Additionally, most massive galaxies are gas-rich (i.e. blue) at high redshift ($z \gtrsim 1$) (Cooper et al. 2007; Gerke et al. 2007; Hopkins et al. 2008), possessing enough gas to be actively star forming. Thus, we anticipate that most, if not all, mergers we track have the capacity to drive galaxy activity such as starbursts and quasars.

2.2 Merger Criteria

We select a subhalo as a major merger (henceforth merger) if its two most massive parents, with $M_{\text{inf},2} \leq M_{\text{inf},1}$, satisfy $M_{\text{inf},2}/M_{\text{inf},1} > 1/3$. As mentioned above, galaxy mergers with stellar mass ratios closer than 3:1 are expected to drive interesting activity, e.g. quasars and starbursts. Unless otherwise stated, we use the shortest simulation output spacing to define the merger time interval, corresponding to 50 Myr (~ 100 Myr) for $M_{\text{inf}} > 10^{11}$ (10^{12}) $h^{-1} M_{\odot}$ at $z > 2.5$, and ~ 200 Myr for all masses at $z < 1.6$.⁵

Other definitions of mergers produce significantly different merger samples. In related work, which inspired our investigation, Thacker et al. (2006) used a dark matter plus hydrodynamic simulation to measure the small-scale clustering of subhalos with recent large mass gains, finding that these subhalos have enhanced small-scale clustering relative to a population with the same large-scale ($\gtrsim 1 h^{-1} \text{Mpc}$) clustering. Mass gain is convenient in that it does not require histories beyond the previous time step, and mass gain is unambiguously defined for all subhalos. However, using our simulations and subhalo finder, the resulting sample is almost entirely different from the one defined above.⁶ Specifically, using a mass gain merger definition in our simulations

led to ‘mergers’ where the two contributing galaxies almost always remained as distinct entities after the merger event. The most common instance of major mass gain is a satellite subhalo gaining mass during its movement within its host halo, particularly as it moves away from the halo center (see Fig. 2 in Paper I and Diemand et al. (2007) for examples). A subhalo can also gain mass by stripping material from the outskirts of a nearby subhalo. In 75% of the cases of major mass gain, one of the progenitors contributed less than 10% of its mass to the resulting ‘merged’ child. The most bound particles (where we expect the stellar material of galaxies to mostly reside) were unaffected. We did find significantly increased small-scale clustering for these mass gain subhalos, attributable to the remaining nearby subhalo which just ‘merged’ with it. Similar issues in using mass gains to define mergers were noted in Maulbetsch et al. (2007).

3 SMALL-SCALE SPATIAL CLUSTERING

When examining the effects of recent mergers on spatial clustering it is important to define an appropriate comparison sample. We have chosen all subhalos above the same given infall mass cut as the mergers, with a matched M_{inf} distribution. We match M_{inf} to remove any possible artificial biasing from, e.g. mergers preferentially occurring for subhalos of higher mass. Using only a mass cut without matching the mass distribution leads to a similar (but weaker) effect. If infall mass is a good proxy for stellar mass, our merger and comparison samples correspond to populations matched in stellar mass.

To measure the small-scale ($\sim 100 - 1000 h^{-1} \text{kpc}$) clustering of subhalo mergers relative to the clustering of the general subhalo population, we measure the cross-correlation function⁷ of the merged and general population, ξ_{mg} , and the auto-correlation function of the general population, ξ_{gg} . Our limited volume unfortunately does not allow us to sub-divide our simulation to measure the sample variance error. For orientation we show $\sqrt{N_{\text{pair}}}$ errors on the correlation function points, but we caution that this may underestimate the error by up to a factor of 2. Our clustering measurements are limited on small scales by the force resolution and on large scales by the simulation volume. We present results on scales where these effects are minor. We shall further discuss the effects of finite simulation volumes and the statistics of massive halos in §4.3.

Figure 1 shows the spatial clustering of recently merged subhalos and the general subhalo population at $z = 2.6$, for two mass regimes and several merger time intervals. These results are representative of our results at other redshifts. Over the smallest time intervals, both high and low mass subhalos have a rise and a decline relative to the general population, with the rise being most prominent for higher mass subhalos and the decline most prominent for lower mass subhalos. For $M_{\text{inf}} > 10^{11} h^{-1} M_{\odot}$, we find an upper limit of $1.8\times$ enhancement at $70 h^{-1} \text{kpc}$, increasing to

⁴ Using the Millennium simulation (Springel et al. 2005), Kitzbichler & White (2008) require an analytic model for satellite infall times after subhalo disruption to match small-scale galaxy clustering at $z \sim 0$. We do not expect this numerical disruption to significantly bias our results since our $100 h^{-1} \text{Mpc}$ simulation has higher mass and temporal resolution.

⁵ This gives 280 (490) mergers at $z = 2.6$ ($z = 1$) above the lower mass cut in our smaller, higher resolution simulation.

⁶ For $M_{\text{inf}} > 10^{11} h^{-1} M_{\odot}$ subhalos at $z = 2.6$, 492 subhalos have $M_{\text{cont},2}/M_{\text{cont},1} > \frac{1}{3}$, compared to the 260 for our infall

mass ratio definition, with only 7 in the intersection of the two sets.

⁷ Not only is the cross-correlation of the mergers with the general population interesting in itself, but it also provides better statistics.

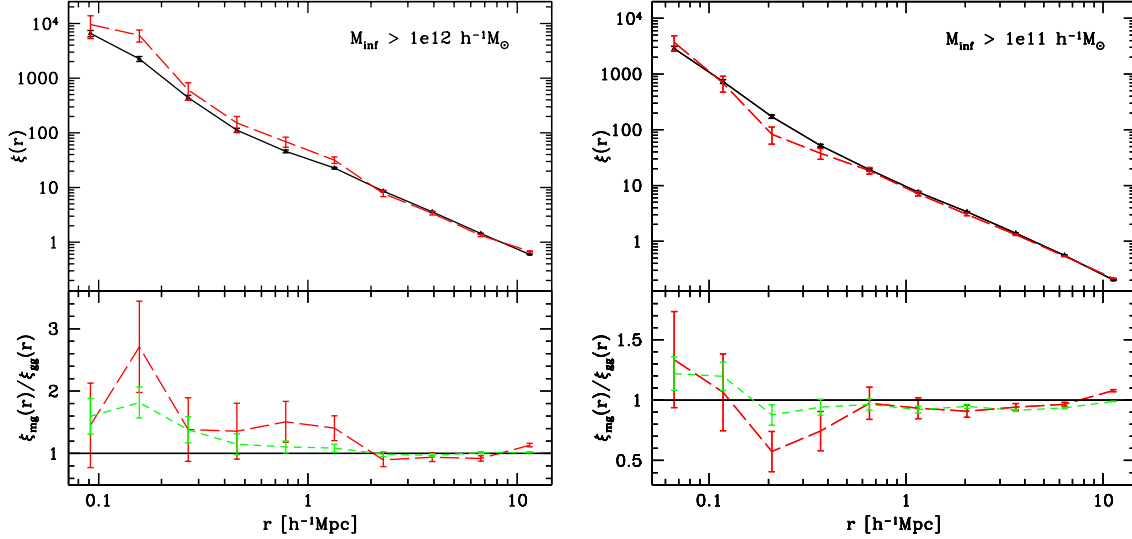


Figure 1. Cross-correlation of recently merged subhalos with all subhalos, $\xi_{mg}(r)$, and the auto-correlation of all subhalos, $\xi_{gg}(r)$, at $z = 2.6$, for $M_{\text{inf}} > 10^{12} h^{-1} M_{\odot}$ (left) and $M_{\text{inf}} > 10^{11} h^{-1} M_{\odot}$ (right). Infall mass, M_{inf} , is matched between the merged and full subhalo samples. **Top Left:** $\xi_{mg}(r)$ for subhalos merging within the last 130 Myr (dashed red) and $\xi_{gg}(r)$ for all subhalos (solid black). **Bottom Left:** Ratio of the cross- and auto-correlations above, for mergers within the last 130 Myr (long-dashed red) and 500 Myr (short-dashed green). **Top Right:** $\xi_{mg}(r)$ for subhalos merging within the last 50 Myr (dashed red) and $\xi_{gg}(r)$ for all subhalos (solid black). **Bottom Right:** Ratio of the cross- and auto-correlations above, for mergers within the last 50 Myr (long-dashed red) and 250 Myr (short-dashed green). Higher mass subhalos show stronger enhanced clustering from mergers, but at both masses no signal persists for subhalos > 500 Myr after merging. Errors are given by $\sqrt{N_{\text{pair}}}$ and do not include sample variance.

$3\times$ that of the general population at $\sim 150 h^{-1} \text{kpc}$ for $M_{\text{inf}} > 10^{12} h^{-1} M_{\odot}$. In addition, lower mass subhalos exhibit a deficit at $100\text{--}300 h^{-1} \text{kpc}$. The enhancement/deficit declines rapidly with the time since the merger, and we see no signal > 500 Myr after the merger. As time progresses central mergers will become satellites in larger halos and satellite mergers will move within their host halos (and perhaps merge with the central) washing out the correlation between the merger and its halo properties that we see at the time of the merger.

4 HALO OCCUPATION DISTRIBUTION AND RADIAL PROFILE

The halo model (Peacock & Smith 2000; Seljak 2000; Cooray & Sheth 2002) can provide insight into the observed clustering signals of the merged subhalo population in Fig. 1. In this framework, galaxies populate dark matter halos such that their large-scale spatial clustering is determined primarily by the clustering of their host dark matter halos (“2-halo term”), while their small-scale spatial clustering arises from galaxies in the same host halo (“1-halo term”). The objects occupy dark matter halos according to a Halo Occupation Distribution (HOD), and have some radial profile within these halos. Since the clustering of recently merged galaxies differs from that of all galaxies, we expect mergers to differ from the general galaxy population in their HOD and/or profile.

4.1 HOD of Subhalos

Figure 2 shows the HOD of subhalos (central and satellite) above $M_{\text{inf}} > 10^{12} h^{-1} M_{\odot}$ at $z = 2.6$ (corresponding to the left hand side of Fig. 1) for all subhalos, recently merged subhalos, and for all subhalos within a halo containing a recently merged subhalo. We see clearly that halos hosting subhalo mergers tend to have more subhalos. This increase occurs for both our high and low mass samples and for all redshifts we probe. For massive subhalo mergers the increase is larger and tends to rise to larger halo mass, which enhances the cross-correlation for mergers. Although lower mass subhalo mergers also have more subhalos per halo, the relative number does not increase with increasing halo mass – host halo mass does not significantly influence merger statistics.

Note that we expect some increase in the number of subhalos above a given mass from mergers of subhalos just below the mass threshold, while mergers between subhalos above the threshold will decrease the number of subhalos. Which effect wins out requires detailed simulations such as ours.

4.2 Central and Satellite Cross-Correlation

We now distinguish between contributions from satellite and central subhalos to the correlation function and HOD of mergers and the general population. There are inherent subtleties in this breakdown; as mentioned earlier, the identification of satellite vs. central subhalos is not entirely clear-cut at these masses and redshifts. In particular, one type can switch to another, and does quite often for mergers (see Paper I for more detail).

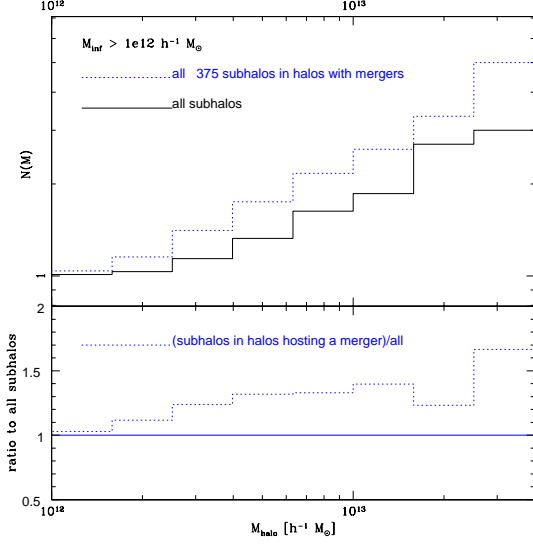


Figure 2. **Top:** Halo Occupation Distribution (HOD) at $z = 2.6$ for all subhalos with $M_{\text{inf}} > 10^{12} h^{-1} M_{\odot}$ (solid black) and subhalos in a halo hosting a recently merged subhalo (dotted blue). The merger time interval is 130 Myr. **Bottom:** Ratio of the HOD of subhalos in a halo hosting a merger to that for all subhalos (dotted blue). There are more subhalos in halos with recently merged subhalos. For recently merged massive subhalos, which show an increase in small-scale clustering, the relative subhalo excess in halos with mergers tends to also increase with halo mass.

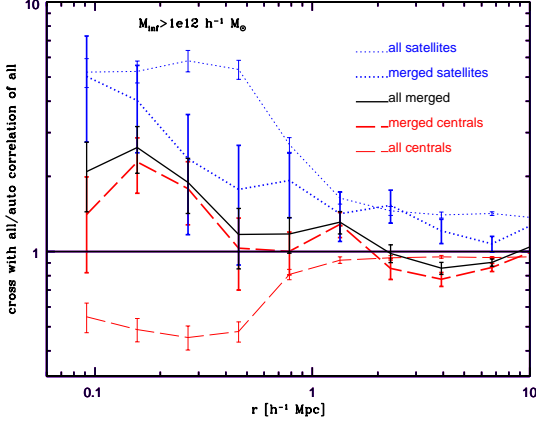


Figure 3. The cross-correlation of the component populations (merged and all satellites, merged and all centrals) with all subhalos (the latter with M_{inf} matched distribution), at $z = 2.6$ for $M_{\text{inf}} > 10^{12} h^{-1} M_{\odot}$, corresponding to the left hand panel of Fig. 1. Top to bottom at far left are $\xi_{\text{sat}} - \text{all} / \xi_{\text{all}}$, $\xi_{\text{sat,merged}} - \text{all} / \xi_{\text{all}}$, $\xi_{\text{all,merged}} - \text{all} / \xi_{\text{all}}$, $\xi_{\text{cen,merged}} - \text{all} / \xi_{\text{all}}$, $\xi_{\text{all}} - \text{all} / \xi_{\text{all}}$, $\xi_{\text{cen}} - \text{all} / \xi_{\text{all}}$.

Figure 3 shows the ratios of the cross-correlations for central mergers and satellite mergers to the auto-correlation of the full sample (the left hand side of Fig. 1 above), for $M_{\text{inf}} > 10^{12} h^{-1} M_{\odot}$ subhalos at $z = 2.6$. The ratios of the cross-correlations of the full central and satellite populations to the full subhalo population are also shown. As before, the full population is matched in M_{inf} to the merged population. In general, satellites have a larger cross-correlation

with all subhalos compared to centrals because the minimum host halo mass for a subhalo of a given mass is larger for a satellite than a central subhalo (increasing the large-scale clustering), and a satellite will always have a central in its halo but not vice versa (increasing the small-scale clustering). The satellite and central cross-correlations must be summed, weighted by their population’s fraction of the full population to get the full cross-correlation.

The merged central and merged satellite contributions to the cross-correlation differ from their counterparts in the full population. Generally, the merged satellites have decreased small-scale clustering, relative to all satellites, while merged centrals have enhancement relative to all centrals. In addition, satellites comprise a larger fraction of the merger population than of the full subhalo population (typically $\sim 1.5 - 2\times$ larger, see Paper I for more discussion), i.e. $N_{\text{sat,merged}}/N_{\text{cen,merged}} \neq N_{\text{sat}}/N_{\text{cen}}$, changing the relative weights satellite and central contributions in the full cross-correlation.⁸ These three trends persist at all redshifts and subhalo mass cuts, but their relative strengths vary to give the different behavior seen in Fig. 1 for different subhalo mass cuts.

4.3 Central and Satellite HOD

We can employ this central/satellite split for the HODs as well. In Fig. 4 we show the HODs for two mass ranges and two redshifts. At left is the HOD for massive ($M_{\text{inf}} > 10^{12} h^{-1} M_{\odot}$) subhalo mergers at $z = 2.6$, corresponding to Fig. 1 (left). At right is the HOD corresponding to the less massive ($M_{\text{inf}} > 10^{11} h^{-1} M_{\odot}$) subhalos at $z = 1$, for a longer (230 Myr) merger time interval. The cross/auto-correlation ratio for this latter sample is similar to that shown in Fig. 1 (right) and is included to illustrate the trends we see over a larger host halo mass range.

Fig. 4 left shows that *high-mass* recently merged central subhalos occupy halos with an excess of satellites (relative to the average) at most host halo masses (the dot-dashed magenta line lies above the dashed black line in the top panel). The physical extent of the enhancement, $\sim 300 h^{-1} \text{kpc}$, coincides with the virial radius of the most massive halos ($\sim 4 \times 10^{13} h^{-1} M_{\odot}$) in our simulations at $z \sim 2.6$. The enhancement of the satellite population in halos hosting recent central mergers is not as large for lower subhalo masses, corresponding to the weakened enhancement, and decrement, in Fig. 1. In terms of the central/satellite subhalo breakdown, the increased satellite number for recently merged central subhalos seems to have the strongest correspondence with increased small-scale clustering.

The other trends we see appear across mass scales and redshifts. For a fixed subhalo mass cut the fraction of centrals that have experienced a recent merger increases with halo mass. This causes an enhancement of the central merger cross-correlation with the full population, since the rise in central merger fraction with halo mass gives the overall recently merged central population proportionally more satellites when all halo masses are summed.

⁸ Since satellites preferentially reside in higher mass halos, if the recently merged population is comprised of a higher fraction of satellites, it will also exhibit the enhanced large-scale clustering.

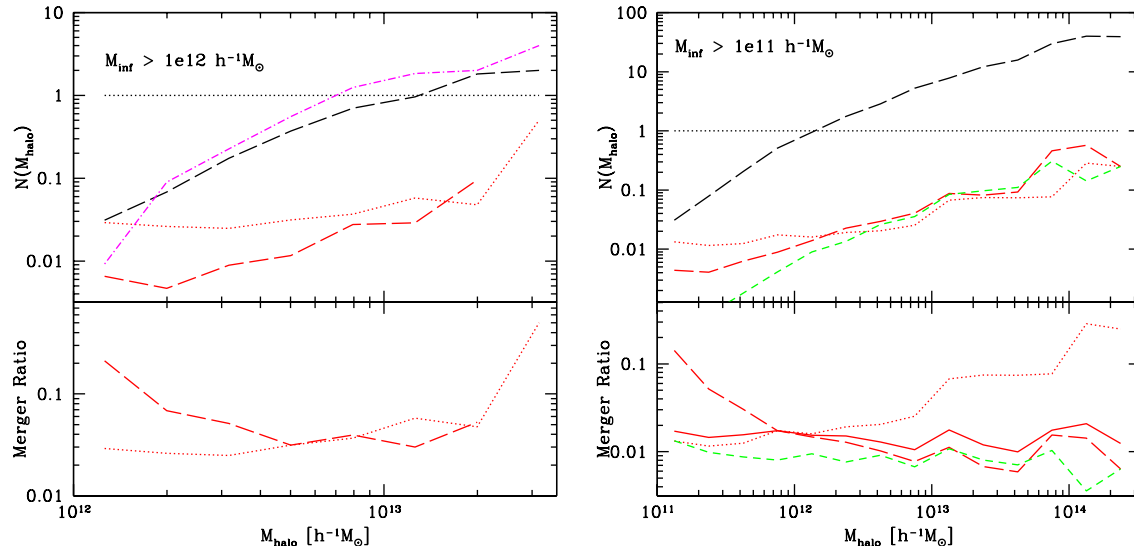


Figure 4. Halo Occupation Distribution (HOD), broken down in terms of merger types: centrals (dotted black), satellites (dashed black), recently merged centrals (dotted red), and recently merged satellites (dashed red). **Top Left:** Subhalos with $M_{\text{inf}} > 10^{12} h^{-1} M_{\odot}$ at $z = 2.6$, corresponding to the left hand side of Fig. 1 and the component contributions in Fig. 3. The merger time interval is 130 Myr. Also shown is the HOD for satellites in halos with a recently merged central (dot-dashed magenta). **Bottom Left:** Ratio of HOD's of recently merged centrals to all centrals (dashed red) and of recently merged satellites to all satellites (dotted red). **Top Right:** Subhalos with $M_{\text{inf}} > 10^{11} h^{-1} M_{\odot}$ at $z = 1$ and mergers occurring within 230 Myr, with cross-correlation similar to the 250 Myr interval in Fig. 1 right at $z = 2.6$. The HOD is also shown for satellite-satellite mergers (short-dashed green). No strong excess is seen for satellites in halos with a recently merged central. **Bottom Right:** Ratio of HOD's of recently merged centrals to all centrals (long-dashed red), recently merged satellites to all satellites (dotted red), and satellite-satellite mergers to all satellites (short-dashed green). Also shown is the ratio of HOD's of subhalo mergers to all subhalos (regardless of type). Satellite-satellite mergers, and subhalo mergers (regardless of type), show no strong dependence on halo mass, though our statistics are not sufficient to rule out a cutoff at the highest mass.

It is worth noting two points about the relative increase of central mergers in higher mass halos. The increase itself might be surprising, as both the number of satellites and the dynamical friction timescale increase approximately linearly with halo mass. One expects that the increase of possible satellites and the slowdown of their approach to the center would then cancel, rather than producing increased numbers of central mergers. Looking instead at merger parent types, we found that the central-satellite merger HOD does not increase as steeply as the merged central HOD. Central mergers in the highest mass halos are often satellite-satellite mergers whose child is a central (switches), rather than central-satellite mergers. While this is a small fraction (3%) of all central mergers, it is a larger fraction of those in high-mass halos.

Secondly, the increase of central mergers to higher mass halos suggests a possible error from neglecting high mass halos which are too rare to occur in the simulation volume. Their effect can be estimated analytically by extrapolating the central merger fraction as a function of halo mass, using the halo model to find the relative contribution of merged and all centrals to the cross-correlation at some given radius, and seeing how this changes as larger masses are included. We find that, on average, neglecting halos more massive than those found in our simulations only causes a small change in the cross-correlation of centrals with the full population. However, our largest halos are quite rare, and so the merger fraction in them does not always tend to the average. The rise in central merger fraction with halo mass is largest for

our $M_{\text{inf}} > 10^{11} h^{-1} M_{\odot}$ subhalos and thus of most concern. As a check, we averaged our cross-correlation for the smaller simulation over several outputs to confirm the trends we see in Fig. 1 (right). The output to output variation does average to this trend, but individual outputs can show different sign effects, albeit with significant error bars. This is especially true at lower redshift, where our imperfect sampling of high mass halos plays a larger role. It might be counterintuitive that $300 h^{-1} \text{kpc}$ clustering is not very well measured in a $100 h^{-1} \text{Mpc}$ box, but the peak of the power spectrum is at large scales in a ΛCDM model and the scatter in the cross-correlation is driven by the contribution from rare, massive halos which host many satellites.

We now turn to the satellite HOD. Figure 4 shows that the fraction of merged satellites to all satellites decreases with increasing host halo mass. However, a significant fraction of merged satellites are satellite-central switches, which dominate in low-mass halos where a central and satellite are more likely to be comparable in mass and thus able to switch. Additionally, some merged satellites are central-satellite mergers which then fell into the host halo. Examining instead merger parent type, satellite-satellite mergers are essentially a constant fraction of satellite subhalos across all halo masses. We see a slight increase for massive hosts at $z = 2.6$ and no increase at $z = 1$, though our statistics at the highest mass are not sufficient to rule out a cutoff at the highest mass.

A simple argument can be made which reproduces the observed scaling of the number of satellite-satellite merg-

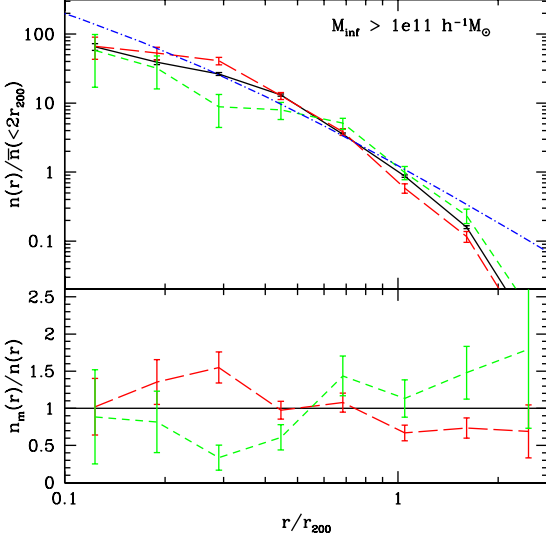


Figure 5. Top: Halo radial distribution profile of satellites with $M_{\text{inf}} > 10^{11} h^{-1} M_{\odot}$ at $z = 2.6$, for all satellites (solid black), recent mergers (long-dashed red), and mergers from satellite-satellite parents (short-dashed green). The merger time interval is 50 Myr. Also shown is the halo NFW density profile (dot-dashed blue). Density distributions are normalized to the average density of the population within $2r_{200c}$. **Bottom:** Ratio of the recently merged satellite normalized density to that of all satellites (long-dashed red) and the same for recent mergers from satellite-satellite parents (short-dashed green). Similar trends persist at higher satellite mass and lower redshift.

ers with the overall satellite population, based upon the HOD scaling with increasing halo mass/volume. For satellites with random orbital parameters in a halo of a fixed mass, the satellite-satellite merger probability will scale as number density squared (n_{sat}^2), so the fraction of satellites undergoing satellite-satellite mergers scales as n_{sat} . For halos above a few times the mass of a given satellite population, the number of satellites scales with the halo mass (e.g., Kravtsov et al. 2004), which scales approximately with the halo volume, so $N_{\text{sat}} \propto M_{\text{halo}} \propto V_{\text{halo}}$. Thus, $n_{\text{sat}} \approx$ constant, so the satellite-satellite merger fraction remains roughly constant. We do see weak evidence for a cutoff in the satellite-satellite merger HOD for the most massive halos, consistent with the idea that increasing relative velocities of satellites in the most massive halos cuts off satellite-satellite mergers (Makino & Hut 1997). However, the high-mass halo statistics are poor in our modest simulation volumes.

Finally, the lower right panel of Fig. 4 shows that when we do not split by type, the subhalo merger fraction is essentially independent of halo mass. Again, this is at odds with frequently expressed intuition that mergers are less frequent in high mass halos, though we caution that our statistics become poor for cluster-sized halos and we are working at high z .

4.4 Radial Distribution Profile

Figure 5 shows the other ingredient required to predict clustering: the (stacked) satellite radial distribution profile, in this case at $z = 2.6$ for subhalos with $M_{\text{inf}} > 10^{11} h^{-1} M_{\odot}$

and a merger time interval of 50 Myr. We choose this mass regime and redshift because the high temporal resolution allows us to accurately identify the locations of mergers, though the behavior across all our mass and redshift regimes is consistent with these results. Shown are the profiles for all satellites, recently merged satellites, recently merged satellites from satellite-satellite parents (because of switches), and the NFW (Navarro et al. 1996) halo density profile. We normalize the density distributions to the average value within $2r_{200c}$. (We calculate r_{200c} by assuming an NFW profile for the given halo mass but use $2r_{200c}$ because an appreciable fraction of satellite mergers occur just outside r_{200c} given the highly aspherical geometry of halos at this mass and redshift regime.) The satellite subhalo profile well-traces the NFW profile from r_{200c} down to $0.2r_{200c}$, consistent with the distribution of subhalos selected on infall mass at $z = 0$ of Nagai & Kravtsov (2005). The deficit below $0.2r_{200c}$ is a result of finite spatial resolution, tidal disruption of subhalos near the halo center, and subhalos temporarily disappearing from the sample during a fly-by (see Fig. 1 of Paper I).

As Fig. 5 shows, the radial distribution profile of satellite mergers approximately follows that of the entire satellite population. The profile can be thought of as a measure of how satellite mergers correlate with centrals, bearing in mind that the distances are scaled by the halo virial radius. Relative to the density distribution of all satellites, recently merged satellites have a slightly more concentrated profile, with enhanced probability of being at 20%–40% of the virial radius (long-dashed red). This produces a relative deficit in clustering of recently merged satellites out to the halo virial radius. Considering instead recently merged centrals, we find that the profile of satellites in halos with a recently merged central trace the general satellite population without significant deviation (not shown).

While recently merged satellites exhibit a slightly more concentrated profile, Fig. 5 shows that mergers between satellite-satellite subhalos preferentially occur in halo outskirts and are comparatively less common in the central regions (short-dashed green). Thus, the enhanced probability of finding recent satellite mergers at small scales is driven by switches (when a satellite merges with a central and results in a satellite).

Finally, we note that other tracking schemes might alter the relation between central and satellite assignments we use here. If switched satellite mergers are assigned as centrals, this will of course not change the observed clustering signal but would alter where the contribution from our switches shows up in the breakdown of central and satellite effects.

5 MERGER PAIRS

While we have focused on measuring merger clustering via the cross-correlation of mergers with the general population, we can also measure directly the statistics of our limited number of merger pairs and distinguish the different origins for the pair members. We focus on pairs of subhalos within $250 h^{-1} \text{kpc}$ which have both undergone a merger within the last ~ 250 Myr. In all such cases of close merger pairs, both subhalos inhabit the same halo. These pairs are quite rare: at $z = 2.6$, there are 24 (2) per $(100 h^{-1} \text{Mpc})^3$ for $M_{\text{inf}} > 10^{11} (10^{12}) h^{-1} M_{\odot}$, while at $z = 1$ there are 2

per $(100 h^{-1} \text{Mpc})^3$ for $M_{\text{inf}} > 10^{11} h^{-1} M_{\odot}$ and none at the higher mass.

For two subhalos within the same halo, the two types of possible pairings are satellite-central and satellite-satellite. For $M_{\text{inf}} > 10^{12} h^{-1} M_{\odot}$, all pairs are composed of satellite-central subhalos, while for $M_{\text{inf}} > 10^{11} h^{-1} M_{\odot}$, 25% of close merger pairs are satellite-satellite subhalos. In all cases, the central-satellite pairs arise when a satellite-central merger occurs simultaneously with a satellite-satellite merger in a single halo. For the rarer cases of satellite-satellite merger pairs, two-thirds of the recently merged satellite arise from a satellite-satellite parents within a halo, and one third arise from a satellite-central merger (a switch).

6 SUMMARY AND DISCUSSION

Using high-resolution dark matter simulations in cosmological volumes, we have measured the small-scale spatial clustering for massive subhalo mergers at high redshift and compared against the clustering of the general subhalo population of the same mass. We have described the merger populations in terms of their HOD and radial profile, including the contributions of centrals vs. satellites. We assign subhalos their mass at infall, as a proxy for galaxy stellar mass, but make no further attempt to model the baryonic component. We consider mergers with $< 3:1$ infall mass ratios, motivated by the expectation that these can trigger activity such as quasars or starbursts. Our main results are:

- At $z = 2.6$, recently merged, massive ($M_{\text{inf}} > 10^{12} h^{-1} M_{\odot}$) subhalos exhibit enhanced small-scale clustering compared to random subhalos with the same infall mass distribution. This excess peaks at $100 - 300 h^{-1} \text{kpc}$, while the clustering exhibits a dip at slightly larger scales. Lower mass subhalos ($M_{\text{inf}} > 10^{11} h^{-1} M_{\odot}$) exhibit signs of a small rise in clustering at $< 100 h^{-1} \text{kpc}$, with a deficit at slightly larger scales, though our results are noisy in this regime. We find similar behavior at $z = 1$. The merger signal weakens rapidly with time, vanishing for time intervals longer than 500 Myr after the merger.

- Considering their HOD, halos hosting recently merged subhalos tended to have more subhalos. This enhancement is stronger for more massive subhalos and exhibited growth with halo mass.

- Breaking the contributions to the cross-correlation into those from satellite and central subhalos, the recently merged massive centrals, which show the largest enhancement of small-scale clustering, preferentially occupy halos with more satellites. More generally, recently merged centrals occupy higher mass halos and recently merged satellites occupy lower mass halos with fewer (perhaps no other) satellites. The resulting increase for the central cross-correlation, decrease for the satellite cross-correlation, and change in the ratio of their contributions combine to produce the cross clustering enhancement or decrement.

- For the range of halo masses we probe, the (type-independent) subhalo merger fraction is independent of host halo mass. We find similar behavior for the halo mass dependence of satellite-satellite mergers, i.e. the fraction of satellites that experience a merger with another satellite does not depend on halo mass, except perhaps in our poorly sampled largest mass halos ($\sim 10^{14} h^{-1} M_{\odot}$).

- The radial profile of recently merged satellites roughly follows that of the entire satellite population, which also follows the halo density profile out to the virial radius. Satellite-satellite mergers preferentially occur in the outer regions of a halo.

- Mergers defined via major mass gain exhibit a strong small-scale clustering enhancement because significant mass gain is caused by interactions with a neighboring subhalo. However, in these cases the neighbor exists both before and after the ‘merger’ (i.e., no coalescence), and the major mass gain criterion does not correspond to dynamically disturbed subhalos. Thus, we do not expect these objects to correlate with active galaxies.

Our measured subhalo merger enhancement suggests that, for populations with the same stellar mass at high redshifts, recent galaxy mergers should exhibit excess clustering at small radius, with a possible decrement in clustering at slightly larger scales. This effect will persist for only a short period of time after the merger, with a stronger excess signal for galaxies of higher stellar mass. Measuring this small-scale cross-correlation (against a general population) requires a surprisingly large volume ($\gtrsim 100 h^{-1} \text{Mpc}$) because massive (satellite rich) halos contribute significant signal to the cross-correlation. A fair sample of rich halos is necessary for robust conclusions.

A comparison of the clustering of our mergers to observational phenomena is a nontrivial future step, since many merger observables depend on complex gas physics. Our results do not include whether the subhalos are gas-rich or not, though at the high redshifts we examine, we expect almost all galaxies to be gas-rich. Satellites can be stripped of much of their gas during infall (e.g., Dolag et al. 2008; Saro et al. 2008), though we have considered relatively massive satellites which have short infall times and thus experience less gas stripping.

Time scales for observables after a merger also have large uncertainty and scatter. For example, an optical quasar might appear only ~ 1 Gyr after the merger (Hopkins et al. 2008; Springel et al. 2005, e.g.), by which time the enhanced clustering that we see has disappeared. X-ray signals might appear sooner.⁹ Starbursts or starburst-related objects (e.g., sub-millimeter galaxies, Lyman break galaxies, ULIRGs) might also commence more rapidly after a merger (e.g., Cox et al. 2008) and thus appear a more promising analog to the effects we find here.

While we were preparing this work for preparation Angulo et al. (2008) appeared which also considers the host halos of satellite mergers in the Millennium simulation.

We thank the participants of the CCAPP workshop on AGN and cosmology for discussions, and especially Phil Hopkins, Alexie Leauthaud, Evan Scannapieco, Francesco Shankar, and Jeremy Tinker. We also thank the CCAPP of The Ohio State University for hospitality in fall 2007. A.W. gratefully acknowledges the support of an NSF Graduate Fellowship, J.D.C. support from NSF-AST-0810820 and DOE, and M.W. support from NASA and the DOE. The simulations were analyzed at the National Energy Research Scientific Computing Center.

⁹ We thank F. Shankar for suggesting this.

REFERENCES

- Angulo R. E., Lacey C. G., Baugh C. M., Frenk C. S., 2008, ArXiv e-prints
- Barnes J. E., Hernquist L. E., 1991, ApJ, 370, L65
- Berrier J. C., Bullock J. S., Barton E. J., Guenther H. D., Zentner A. R., Wechsler R. H., 2006, ApJ, 652, 56
- Blain A. W., Chapman S. C., Smail I., Ivison R., 2004, ApJ, 611, 725
- Blain A. W., Smail I., Ivison R. J., Kneib J.-P., Frayer D. T., 2002, Phys. Rep., 369, 111
- Bower R. G., Benson A. J., Malbon R., Helly J. C., Frenk C. S., Baugh C. M., Cole S., Lacey C. G., 2006, MNRAS, 370, 645
- Carlberg R. G., 1990, ApJ, 350, 505
- Coil A. L., Hennawi J. F., Newman J. A., Cooper M. C., Davis M., 2007, ApJ, 654, 115
- Conroy C., Wechsler R. H., 2008, ArXiv e-prints, 805
- Conroy C., Wechsler R. H., Kravtsov A. V., 2006, ApJ, 647, 201
- Cooper M. C., Newman J. A., Coil A. L., Croton D. J., Gerke B. F., Yan R., Davis M., Faber S. M., Guhathakurta P., Koo D. C., Weiner B. J., Willmer C. N. A., 2007, MNRAS, 376, 1445
- Cooray A., Ouchi M., 2006, MNRAS, 369, 1869
- Cooray A., Sheth R., 2002, Phys. Rep., 372, 1
- Cox T. J., Jonsson P., Somerville R. S., Primack J. R., Dekel A., 2008, MNRAS, 384, 386
- Croom S. M., Boyle B. J., Shanks T., Smith R. J., Miller L., Outram P. J., Loaring N. S., Hoyle F., da Ângela J., 2005, MNRAS, 356, 415
- Croton D. J., Gao L., White S. D. M., 2007, MNRAS, 374, 1303
- Davis M., Efstathiou G., Frenk C. S., White S. D. M., 1985, ApJ, 292, 371
- Diemand J., Kuhlen M., Madau P., 2007, ApJ, 667, 859
- Dolag K., Borgani S., Murante G., Springel V., 2008, ArXiv e-prints, 808
- Francke H., Gawiser E., Lira P., Treister E., Virani S., Cardamone C., Urry C. M., van Dokkum P., Quadri R., 2008, ApJ, 673, L13
- Furlanetto S. R., Kamionkowski M., 2006, MNRAS, 366, 529
- Gao L., Springel V., White S. D. M., 2005, MNRAS, 363, L66
- Gawiser E., Francke H., Lai K., Schawinski K., Gronwall C., Ciardullo R., Quadri R., Orsi A., Barrientos L. F., et al., 2007, ApJ, 671, 278
- Gerke B. F., Newman J. A., Faber S. M., Cooper M. C., Croton D. J., Davis M., Willmer C. N. A., Yan R., Coil A. L., Guhathakurta P. and Koo D. C., Weiner B. J., 2007, MNRAS, 376, 1425
- Ghigna S., Moore B., Governato F., Lake G., Quinn T., Stadel J., 1998, MNRAS, 300, 146
- Giavalisco M., 2002, ARA&A, 40, 579
- Giavalisco M., Steidel C. C., Adelberger K. L., Dickinson M. E., Pettini M., Kellogg M., 1998, ApJ, 503, 543
- Hennawi J. F., Strauss M. A., Oguri M., Inada N., Richards G. T., Pindor B., Schneider D. P., Becker R. H., Gregg M. D., Hall P. B., Johnston D. E., Fan X., Burles S., Schlegel D. J., Gunn J. E., Lupton R. H., Bahcall N. A., Brunner R. J., Brinkmann J., 2006, AJ, 131, 1
- Hopkins P. F., Cox T. J., Kereš D., Hernquist L., 2008, ApJS, 175, 390
- Hopkins P. F., Hernquist L., Cox T. J., Kereš D., 2008, ApJS, 175, 356
- Kashikawa N. e. a., 2006, ApJ, 637, 631
- Kitzbichler M. G., White S. D. M., 2008, ArXiv e-prints, 804
- Klypin A., Gottlöber S., Kravtsov A. V., Khokhlov A. M., 1999, ApJ, 516, 530
- Komatsu E., Dunkley J., Nolte M. R., Bennett C. L., Gold B., Hinshaw G., Jarosik N., Larson D., Limon M., Page L., Spergel D. N., Halpern M., Hill R. S., Kogut A., Meyer S. S., Tucker G. S., Weiland J. L., Wollack E., Wright E. L., 2008, ArXiv e-prints, 803
- Kravtsov A. V., Berlind A. A., Wechsler R. H., Klypin A. A., Gottlöber S., Allgood B., Primack J. R., 2004, ApJ, 609, 35
- Lee K.-S., Giavalisco M., Gnedin O. Y., Somerville R. S., Ferguson H. C., Dickinson M., Ouchi M., 2006, ApJ, 642, 63
- Makino J., Hut P., 1997, ApJ, 481, 83
- Masjedi M., Hogg D. W., Cool R. J., Eisenstein D. J., Blanton M. R., Zehavi I., Berlind A. A., Bell E. F., Schneider D. P., Warren M. S., Brinkmann J., 2006, ApJ, 644, 54
- Maulbetsch C., Avila-Reese V., Colín P., Gottlöber S., Khalatyan A., Steinmetz M., 2007, ApJ, 654, 53
- Moore B., Ghigna S., Governato F., Lake G., Quinn T., Stadel J., Tozzi P., 1999, ApJ, 524, L19
- Myers A. D., Richards G. T., Brunner R. J., Schneider D. P., Strand N. E., Hall P. B., Blomquist J. A., York D. G., 2008, ApJ, 678, 635
- Nagai D., Kravtsov A. V., 2005, ApJ, 618, 557
- Navarro J. F., Frenk C. S., White S. D. M., 1996, ApJ, 462, 563
- Noguchi M., 1991, MNRAS, 251, 360
- Ouchi M., Hamana T., Shimasaku K., Yamada T., Akiyama M., Kashikawa N., Yoshida M., Aoki K., Iye M., Saito T., Sasaki T., Simpson C., Yoshida M., 2005, ApJ, 635, L117
- Padmanabhan N., White M., Norberg P., Porciani C., 2008, ArXiv e-prints, 802
- Peacock J. A., Smith R. E., 2000, MNRAS, 318, 1144
- Percival W. J., Scott D., Peacock J. A., Dunlop J. S., 2003, MNRAS, 338, L31
- Reichardt C. L., Ade P. A. R., Bock J. J., Bond J. R., Brevik J. A., Contaldi C. R., Daub M. D., Dempsey J. T., Goldstein J. H., Holzapfel W. L., Kuo C. L., Lange A. E., Lueker M., Newcomb M., Peterson J. B., Ruhl J., Runyan M. C., Staniszewski Z., 2008, ArXiv e-prints, 801
- Sanders D. B., Mirabel I. F., 1996, ARA&A, 34, 749
- Saro A., De Lucia G., Dolag K., Borgani S., 2008, ArXiv e-prints, 809
- Scannapieco E., Thacker R. J., 2003, ApJ, 590, L69
- Scott S. E., Dunlop J. S., Serjeant S., 2006, MNRAS, 370, 1057
- Seljak U., 2000, MNRAS, 318, 203
- Shen Y., Strauss M. A., Oguri M., Hennawi J. F., Fan X., Richards G. T., Hall P. B., Gunn J. E., Schneider D. P., Szalay A. S., Thakar A. R., Vanden Berk D. E., Anderson S. F., Bahcall N. A., Connolly A. J., Knapp G. R., 2007, AJ, 133, 2222
- Sheth R. K., Tormen G., 2004, MNRAS, 350, 1385

- Smoot G. F., et al., 1992, ApJ, 396, L1
- Springel V., Di Matteo T., Hernquist L., 2005, MNRAS, 361, 776
- Springel V., White S. D. M., Jenkins A., Frenk C. S., Yoshida N., Gao L., Navarro J., Thacker R., Croton D., Helly J., Peacock J. A., Cole S., Thomas P., Couchman H., Evrard A., Colberg J., Pearce F., 2005, Nature, 435, 629
- Springel V., White S. D. M., Tormen G., Kauffmann G., 2001, MNRAS, 328, 726
- Tegmark M., et al., 2006, PRD, 74, 123507
- Thacker R. J., Scannapieco E., Couchman H. M. P., 2006, ApJ, 653, 86
- Tinker J. L., Conroy C., Norberg P., Patiri S. G., Weinberg D. H., Warren M. S., 2008, ApJ, 686, 53
- Tormen G., 1997, MNRAS, 290, 411
- Tormen G., Diaferio A., Syer D., 1998, MNRAS, 299, 728
- Vale A., Ostriker J. P., 2006, MNRAS, 371, 1173
- Wang L., Li C., Kauffmann G., De Lucia G., 2006, MNRAS, 371, 537
- Wechsler R. H., Zentner A. R., Bullock J. S., Kravtsov A. V., Allgood B., 2006, ApJ, 652, 71
- Wetzel A. R., Cohn J. D., White M., 2008, ArXiv e-prints
- Wetzel A. R., Cohn J. D., White M., Holz D. E., Warren M. S., 2007, ApJ, 656, 139
- White M., 2002, ApJS, 143, 241
- Yamauchi C., Yagi M., Goto T., 2008, ArXiv e-prints, 809
- Yan R., Newman J. A., Faber S. M., Coil A. L., Cooper M. C., Davis M., Weiner B. J., Gerke B. F., Koo D. C., 2008, ArXiv e-prints, 805
- Yang X., Mo H. J., van den Bosch F. C., 2008, ArXiv e-prints, 808
- Yoshida M., Shimasaku K., Ouchi M., Sekiguchi K., Furusawa H., Okamura S., 2008, ApJ, 679, 269
- Zentner A. R., Berlind A. A., Bullock J. S., Kravtsov A. V., Wechsler R. H., 2005, ApJ, 624, 505